

# Dispersal-induced resilience to stochastic environmental fluctuations in populations with Allee effect

**Rodrigo Crespo<sup>a</sup>, Francisco J. Cao-García<sup>b</sup>**

<sup>a</sup> Departamento de Estructura de la Materia, Física Térmica y Electrónica, Facultad de Ciencias Físicas, Universidad Complutense de Madrid. Plaza de Ciencias 1, 28040 Madrid, Spain; and Departamento de Física de la Tierra y Astrofísica, Facultad de Ciencias Físicas, Universidad Complutense de Madrid. Plaza de Ciencias 1, 28040 Madrid, Spain. Email: [rodcrep@ucm.es](mailto:rodcrep@ucm.es)

<sup>b</sup> Departamento de Estructura de la Materia, Física Térmica y Electrónica, Facultad de Ciencias Físicas, Universidad Complutense de Madrid. Plaza de Ciencias 1, 28040 Madrid, Spain; and Instituto Madrileño de Estudios Avanzados en Nanociencia (IMDEA-Nanociencia). Calle Faraday 9, 28049 Madrid, Spain. Email: [francao@ucm.es](mailto:francao@ucm.es). Telephone: +34 91 394 4742.

**Corresponding author.**

**Short running title:** Resilience to environmental fluctuations.

**Keywords:** Population resilience; extinction risk; stochastic population dynamics; sustainability; climate variability increase; impact of climate scenarios.

**Autorship statement:** FJCG designed the research, RC performed the numerical computations of the models, analyzed the output, and prepared the figures. Both authors wrote the manuscript.

## **Abstract**

Many species are unsustainable at small population densities (Allee Effect). This implies that for population densities below a threshold, named Allee threshold, the population decreases instead of growing. In a closed local population, this makes that environmental fluctuations always leads to extinction. Here, we show how, in spatially extended habitats, dispersal can lead to a sustainable population in a region, provided the amplitude of environmental fluctuations is below an extinction threshold. We have identified two types of sustainable populations: high-density and low-density populations (through a mean-field approximation, valid in the limit of large dispersal length). Our results show that close to global extinction patches where population density is high, low or extinct coexist (even for homogeneous habitats). The extinction threshold increases proportionally to the squared root of the dispersal rate, decreases with the Allee threshold, and it is maximum for characteristic dispersal distances much larger than the spatial scale of synchrony of environmental fluctuations. The low-density population solution can be particularly interesting for future applications, as to understand non-recovery events after harvesting. This theoretical framework allows novel approaches to address the impact of other factors, as habitat fragmentation, on the population resilience to environmental fluctuations.

### *1. Introduction*

Many species need a minimum population density to be viable such as the island fox (Angulo et al. 2007), the polar bear (Molnár et al. 2008), the american ginseng (Hackney and McGraw 2001) and the atlantic codfish (Kuparinen and Hutchings 2014) among others. This minimum viable population density is named Allee threshold (Allee 1931), and below it, the population declines towards extinction, a phenomenon called the Allee effect.

Field researches have shown the effects of the Allee effect on populations of plants and animals that, for different causes, have decreased below the Allee threshold. The effects depend on the strength of the Allee Effect, on the absence of harvest and on the presence of positive human intervention. Many of these depleted populations never recover and become extinct in some years. Some depleted populations take many years (much more than the average lifetime of the species) to get out of this situation and eventually recover. In animals, monogamous species with long lifetimes tend to be more vulnerable to Allee Effect (Saether et al. 2006; Angulo et al. 2007), in addition to solitary species with difficulties for finding breeding mate or an unbalanced male-female ratio (Molnár et al. 2008). Another causes that can explain Allee effect in animals are non-efficient feeding (Way and Banks 1967), difficulties to survive in an environment with predators, competitors or human harvest (Moynihan and Kruuk 2010; Kenward 2006; Jarillo et al. 2018) or inbreeding (Ralls, Frankham, and Ballou 2013; Frankham and Ralls 1998). In plants, less efficient pollination or fruit production (decreasing at small populations) (Hackney and McGraw 2001) seem to be the principal causes providing Allee Effect. Most of the articles cited above qualitatively describe how a particular species in a low population density situation has difficulties surviving due to Allee Effect.

Theoretical papers have addressed the general question of the eradication of alien species (Liebhold and Bascompte 2003), and of the spatial patterns influence on the spread of invading species (Lewis and Kareiva 1993), observed in gypsy moth (Vercken et al. 2011). These papers show that both the Allee Effect and environmental variability can contribute to the extinction of a population. Other works have studied the effects of stochasticity in species vulnerable to the Allee Effect (Dennis 2002; Engen, Lande, and Sæther 2003; Lee, Sæther, and Engen 2011;

Méndez et al. 2019) describing mean time to extinction, or probability of extinction after a given time, for a single location.

Studies of a locally endangered butterfly sustain the critical role of immigration in the regional dynamics to counterbalance the Allee effects (Bonsall et al. 2014). Recently, Dennis et al. (Dennis et al. 2016) have shown that an external constant migration term can sustain the population in the presence of stochastic environmental fluctuations. Here, we go a step further and show that a spatially extended population with dispersal between the locations can be sustainable. We clarify the conditions for sustainability in spatially extended habitats, quantifying the effects of dispersal in the resilience to stochastic environmental fluctuations.

The results we present here provide insight on how natural or human-induced changes in the species dynamical parameters would influence its extinction risk due to environmental fluctuations. In particular, it provides information on how an increase in the amplitude of environmental fluctuations can affect the sustainability of a population. This problem is of particular present relevance as several regions of the Earth are increasing its climate variability (IPCC 2012).

## **2. Methods:**

### ***2.1. Spatially extended population model***

We introduce here a spatially extended, one-dimensional, population model, including Allee effects, environmental fluctuations, and dispersal. This model allows us to assess the resilience of populations to environmental fluctuations, and the role played by dispersal in this resilience.

The deterministic Allee model (Allee and Rosenthal 1949; Odum and Allee 2006) gives the local deterministic dynamics of the population density  $N(x,t)$ . This dynamics is determined by a

characteristic growth rate  $r$ , a carrying capacity  $K$  (stable viable population density), and an Allee threshold  $A$  (minimum viable population density). Note that the population density  $N(x,t)$  is defined as the local number of individuals per unit of length at a given time. Additionally, environmental stochasticity is introduced through an additional stochastic contribution  $\sigma N dB$ , which is proportional to the population density. The amplitude of these environmental fluctuations is given by  $\sigma$ , and  $dB(x,t)$  is a normalized Gaussian random field with a spatial scale of synchrony  $l_e$ , giving the spatial scale of synchrony of the environmental fluctuations, which is the characteristic distance at which environmental fluctuations remain correlated (Jarillo et al. 2018). Therefore, the local dynamics of a population density  $N(x,t)$  in the stochastic Allee model is given by

$$dN|_{local} = r N (N/A-1) (1-N/K) dt + \sigma N dB \quad (1)$$

The first term corresponds to the deterministic Allee model (Allee and Rosenthal 1949; Odum and Allee 2006). This equation implies a rate of return to extinction for populations close to extinction of  $\gamma_0 = r$  and a rate of return to the carrying capacity for populations close to the carrying capacity of  $\gamma_K = r (K/A-1)$ . The second term in Eq. (1) gives the contribution of stochastic environmental fluctuations to the changes in the local population, with an amplitude of the environmental fluctuations  $\sigma$ . The random field  $dB(x,t)$  is given by increments of standard Brownian motions in each position with zero mean and variance  $dt$ , and it is spatially correlated with an exponential autocorrelation of length  $l_e$ , which is the spatial scale of synchrony of environmental fluctuations (Jarillo et al. 2018).

The dispersal couples the dynamics in the different locations. We consider that individuals disperse away with a rate  $m$  to a characteristic distance  $l_m$ . Thus, dispersal gives an additional contribution to the dynamics of

$$dN|_{dispersal} = -m N dt + m dt \int N(x-y,t) f(y) dy \quad (2)$$

which makes the dynamics non-local. The first term represents the population decrease at position  $x$  due to individuals that disperse away with probability  $m dt$ . The second term gives the population increase due to individuals that disperse to position  $x$  from a position that is at a distance  $y$ , being  $N(x-y,t)$  the population at a distance  $y$ . Therefore,  $m$  is the rate of random dispersal to a position at a distance  $y$  with probability  $f(y)$ , where  $f(y)$  is a Gaussian with variance  $l_m^2$  and zero mean. Hence, individuals disperse at a rate  $m$  to typical distances of the order of  $l_m$ . The combination of both contributions to the change in population density gives the complete spatially extended dynamics,

$$dN = dN|_{local} + dN|_{dispersal} \quad (3)$$

Typical population distributions at long times given by this dynamical equation can be seen in Fig. 1 (panels A, C, and E).

## 2.2. Numerical simulations

The numerical simulations of the previously described dynamical equation is performed taking the scale of synchrony of environmental fluctuations,  $l_e$ , as reference length, *i.e.*,  $l_e=1$ , and 20 lattice nodes per unit length. The total length of the simulation box was 140 times the maximum of  $l_e$  and  $l_m$ , and we consider periodic boundary conditions (aiming to obtain results for infinite habitat). The time resolution was 50 times smaller than the minimum of the characteristic times of the dynamics (*i.e.*, the minimum of the inverses of the rates  $r$  and  $m$ ). These resolutions, simulations boxes, and boundary conditions guarantee that the dynamics is well-resolved in time and space, and that mimics an infinite habitat for better comparison with the results found with the mean-field approximation (Law, Dieckmann, and Metz 2000; Morozov and Poggiale 2012)

described below. In this way, we performed numerical simulations of spatially extended populations, starting from a population density equal to the carrying capacity. We ran several simulations for each set of parameters with different amplitudes of the environmental fluctuations.

We define the extinction threshold,  $\sigma_{extinction}$ , as the amplitude of environmental fluctuations above which the environmental fluctuations lead to the global extinction of population. From these simulations, the environmental fluctuation extinction threshold  $\sigma_{extinction}$  is obtained as the smallest amplitude of the environmental fluctuations for which the population always suffers global extinction at long times ( $t=1000$ ).

Besides, relevant information of a spatially extended population is how probable it is to find a given population density in a given location, *i.e.*, to determine the population probability distribution. Here, the population probability distribution  $p(N)$  does not depend on location, as we have assumed homogeneous habitat conditions, represented by location-independent population dynamics parameters (growth rate  $r$ , carrying capacity  $K$ , Allee threshold  $A$ , and amplitude of environmental fluctuations  $\sigma$ ). Thus, the population probability distribution  $p(N)$  gives the probability to find the population density  $N$ . The population probability distribution  $p(N)$  is computed from numerical simulations doing population density histograms, like those shown in Fig. 1 Panels B, D, and F.

### ***2.3. Analytical population probability distribution***

Additionally, we can get further insight into the population dynamics through a more analytical approach for the computation of the population probability. The stochastic differential equations for the stochastic Allee model with dispersal, Eq. 3, has the form  $= F(N) dt + \sqrt{v(N)} dB$ . For

equations of this form, if a stationary population probability distribution exists it is given by (Karlin and Taylor 1967)

$$p(N) = \frac{n}{v(N)} \cdot \exp\left(2 \int \frac{F(N)}{v(N)} dN\right). \quad (4)$$

Therefore, for the stochastic Allee model with dispersal, Eq. 3, the stationary population probability distribution is

$$p(N) = \frac{n \cdot \exp\left(\frac{1}{\sigma^2} \left(\frac{2rN}{K} + \frac{2rN}{A} - \frac{rN^2}{AK} - \frac{2mI}{N}\right)\right)}{\sigma^2 N^{2+2(r+m)/\sigma^2}}, \quad (5)$$

where  $n$  is the normalization factor, and the coupling term  $I(x) = \int N(x-y) f(y) dy$  makes the population probability in one location depending on the values of the population density in the surrounding region.

#### ***2.4. Mean-field approximation***

We propose here to combine the analytic expression in Eq. (5) with the mean-field approximation to deal with the coupling term  $I(x)$ . When the dispersal length is much larger than the spatial scale of synchrony of environmental fluctuations,  $l_m \gg l_e$ , (for example, the case of long-distance migrant birds) the mean-field approximation is a good approximation. The mean-field approximation assumes the stationary population density is approximately equal in all points of space (because long-distance migration,  $l_m \gg l_e$ , tends to make the population more uniform along all space, recolonizing low-populated points from those that are “overpopulated”). The mean-field approximation implies that the coupling term  $I$  in Eq. (5) can be treated as position independent,  $I(x) = I$ , and we can approximate it by the mean value of the population density

$$I = \int_0^{\infty} N p(N) dN. \quad (6)$$

The extinction threshold,  $\sigma_{extinction}$ , was defined here as the amplitude of environmental fluctuations above which the environmental fluctuations leads to the global extinction of population. In the mean-field approximation, the extinction threshold can be computed directly obtaining the value of the environmental amplitude where there is no longer a solution of the system of equations formed by Eqs. 5 and 6 (*i.e.*, the point where the green and the red curve merge in Fig. 2), except the extinction in all space solution,  $p(N = 0) = 1$ . Therefore, in addition to the possibility of calculating a stationary probability distribution, the mean-field approximation allows us to estimate quickly the extinction threshold for a particular set of parameters (which is a close upper limit of the real extinction threshold when the dispersal distance of the species is large enough). We get two branches of solutions, which represent two different equilibria: the high mean population density solution,  $p_{high}$ , and low mean population density solution,  $p_{low}$ . See Figs. 1 and 2.

### ***2.5. Maximum approximation***

An estimation of the extinction threshold can be obtained adding the maximum approximation, which assumes the extinction threshold is the value of the amplitude of environmental fluctuations  $\sigma$  that locates the maximum of  $p_I(N)$  [where  $p_I(N)$  is the population probability for a given  $I$ ] at the Allee threshold  $A$ . This estimation gives for the extinction threshold

$$\sigma_{extinction} = \sqrt{m \left( \frac{I}{A} - 1 \right)}. \quad (7)$$

Furthermore, this expression is useful to notice that the extinction threshold approximately increases with the square root of the migration rate and decreases with the Allee threshold  $A$

(Fig. 3). In order to obtain the value of  $\sigma_{extinction}$  estimated with the mean-field and maximum approximations, we must simultaneously solve numerically Eqs. 5, 6, and 7.

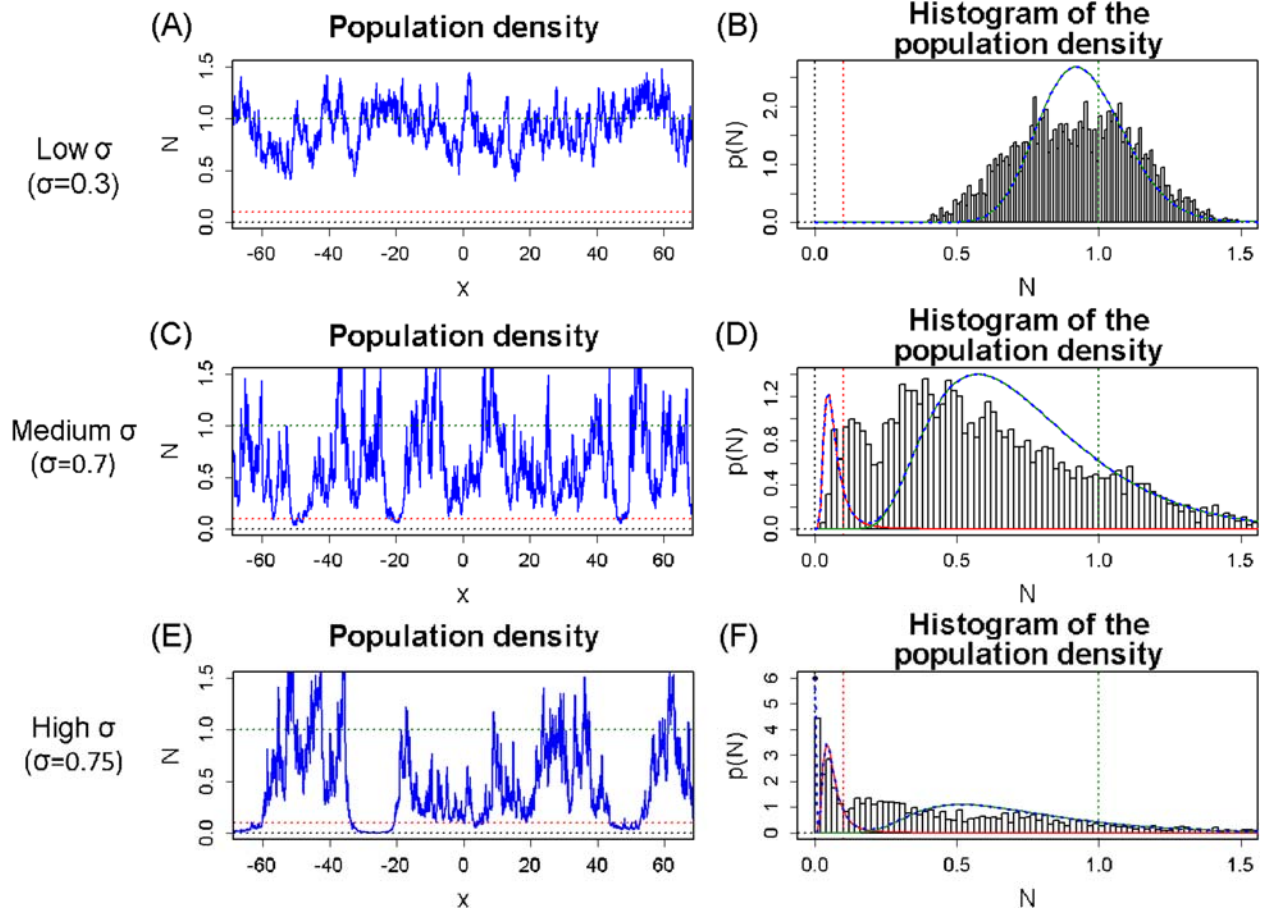


*Fig. 1: Spatial profiles of population density, their associated averaged population density histograms compared with mean-field population probability distributions. Panels A, C and E: spatial profile of the population density for simulation at long time,  $t=1000$ , with growth rate  $r=0.1$ , Allee threshold  $A=0.1$ , carrying capacity  $K=1$ , migration rate  $m=1$ , and migration distance equal to the spatial scale of synchrony of environmental fluctuations,  $l_m=l_e$ . Panels B, D, and F: population density histograms for the spatial profiles of population densities shown in*

Panels A, C, and E, respectively. In Panels B, D, and F, we also show the theoretical population probability distributions given by the two non zero branches of solutions of the mean-field equations for values of  $\sigma$  below the extinction threshold. They correspond to the low and high density population probability distributions solutions (presented in the following section),  $p_{low}(N)$  with a red line, and  $p_{high}(N)$  with a green line, respectively. We represent in the figure these distributions weighted with the coefficients resulting from a fit of a linear combination of them and the zero population density solution  $p_0(N)$  (black point). The result for this fits are  $p(N)=p_{high}(N)$  in Panel B,  $p(N)=0.08p_{low}(N)+0.92p_{high}(N)$  in Panel D and  $p(N)=0.06p_0(N)+0.22p_{low}(N)+0.72p_{high}(N)$  in Panel F. Red dashed lines indicate Allee threshold value  $A=0.1$ , green dashed lines indicate carrying capacity  $K=1$  and black dashed lines indicate  $N=0$ . Note the similarities between the population density histograms obtained from direct numerical simulation and the fit to the linear combination of the population probability distributions obtained with the mean-field limit approximation (i.e., the large migration distance limit,  $l_m/l_e \rightarrow \infty$ ). However, the real histograms are displaced to the left due to the border effects, which are effects beyond the mean-field approximation (i.e., due to finite migration distance, in this case  $l_m/l_e=1$ ). Note also that increasing the environmental fluctuations  $\sigma$  increases the presence of regions where the population is depleted or extinct, as  $\sigma$  approaches the extinction threshold ( $\sigma_{extinction}=0.80$  for the parameter values in this figure).

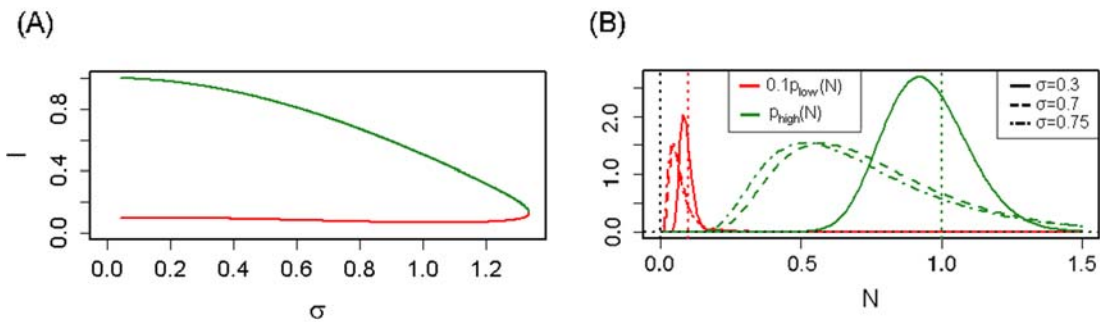


*Fig. 2: Solutions in the mean-field approximation: (Panel A) Mean population density  $I$  as a function of environmental noise amplitude  $\sigma$  for the two non-zero branches of solutions at the mean-field approximation, with growth rate  $r=0.1$ , carrying capacity  $K=1$ , Allee threshold  $A=0.1$ , and migration rate  $m=1$ . (Panel B) High population (green) and low population (red, divided by 10 to make the figure more visible) probability distributions,  $p_{high}$  and  $p_{low}$  respectively, calculated at the mean-field approximation for the same parameters of Panel A, for values of the environmental fluctuations amplitude  $\sigma=0.3$  (solid line),  $\sigma=0.7$  (dashed line) and  $\sigma=0.75$  (dash-dotted line). Vertical lines show  $N=0$  (black),  $N=A=0.1$  (red) and  $N=K=1$ (green). Note that distributions tend to move to lower values of population density as environmental fluctuation amplitude  $\sigma$  increases.*

Variables	Description
$N(x,t)$	Population density at a given position $x$ and a time $t$ . Dimensionless
$A$	Allee threshold of the species, below it, the species has negative growth. Dimensionless.
$K$	Carrying capacity of the species, meaning stable viable population density. Dimensionless
$r$	Growth rate. Units of $\text{time}^{-1}$
$\gamma_0$	Rate of return to extinction. Units of $\text{time}^{-1}$
$\gamma_K$	Rate of return to carrying capacity. Units of $\text{time}^{-1}$
$m$	Dispersal rate of the species. Units of $\text{time}^{-1}$
$l_e$	Spatial scale of synchrony of environmental fluctuations. Units of length

$l_m$	Mean distance traveled by the dispersed individuals (characteristic width of the Gaussian dispersion function). Units of length
$\sigma$	Amplitude of the environmental fluctuations. The standard deviation of the environmental fluctuations gives it. Units of time <sup>-1/2</sup>
$\sigma_{extinction}$	Extinction threshold for the amplitude of environmental fluctuations (Minimum amplitude of the fluctuations that ensures global extinction). Units of time <sup>-1/2</sup>

Table 1: Variables used in this article, definition, and units.

### 3. Results: Dispersal makes the population resilient to environmental fluctuations

In a closed local population, environmental fluctuations lead to extinction in the presence of environmental fluctuation, because environmental fluctuations eventually lead the population density below the Allee threshold  $A$ . Our results show that the presence of dispersal allows the recovery of a region with a depleted population thanks to population arriving from nearby non-depleted regions. This dispersal induced population recovery makes the species resilient to population depletions caused by environmental fluctuations. Resilience to environmental fluctuations increases with the increase of dispersal, both by increasing dispersal rate or by increasing dispersal length. See Fig. 3, where the extinction threshold  $\sigma_{extinction}$  is represented, when environmental fluctuations are more intense than this threshold, the population gets globally extinct.

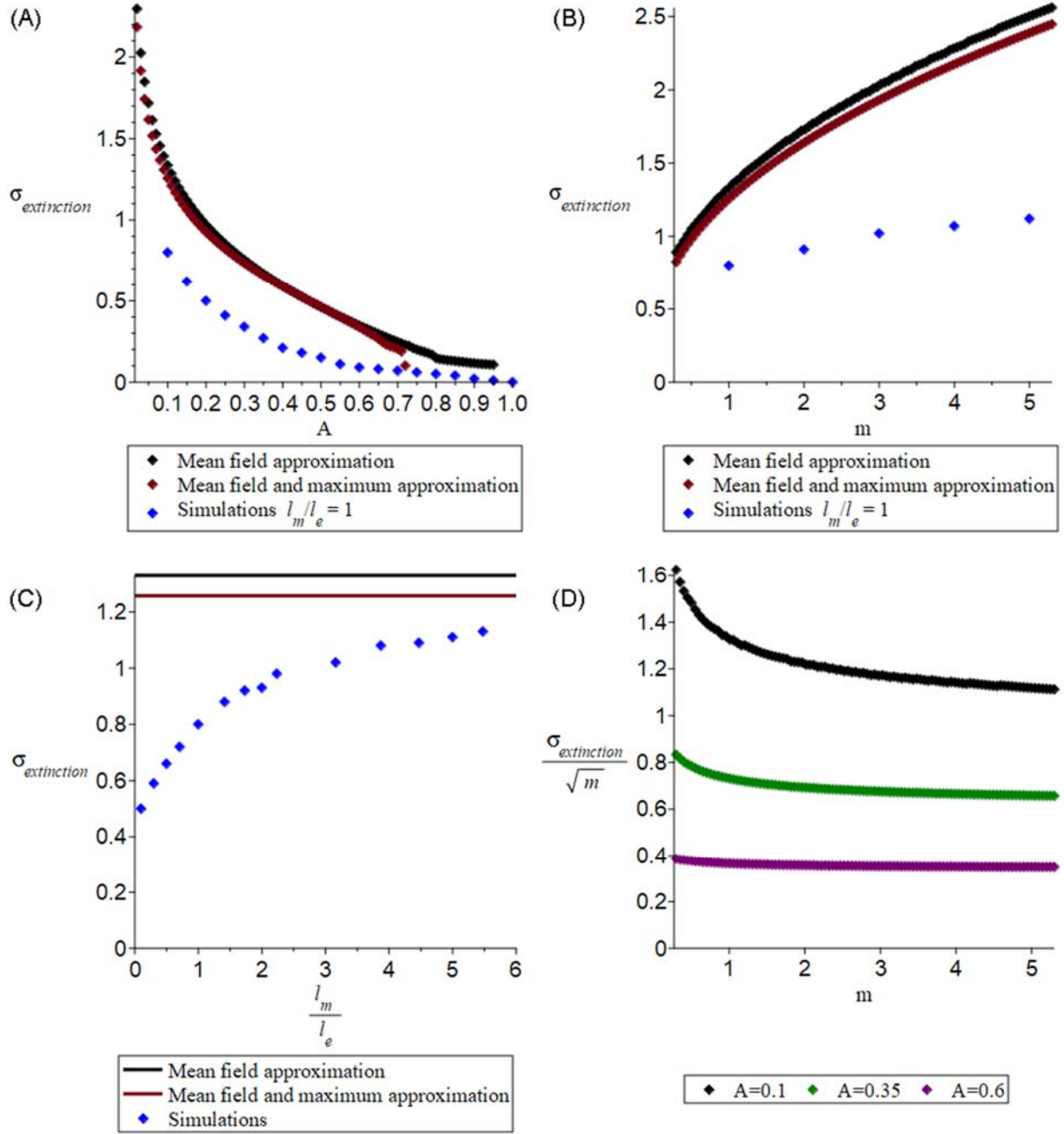


Fig 3: Extinction threshold,  $\sigma_{extinction}$ , versus different parameters. (Panel A) Extinction threshold versus Allee threshold for the mean-field approximation (black dots) (i.e., large migration length,  $l_m \gg l_e$ ), for the mean-field and maximum approximations (red dots), and for a simulation with  $l_m = l_e$  (i.e., migration length  $l_m$  equal to the spatial scale of synchrony of environmental fluctuations  $l_e$ ) all with dispersal rate  $m=1$ . (Panel B) Extinction threshold versus dispersal rate

using the same color code as the previous panel, all with Allee threshold  $A=0.1$ . The migration rates considered vary from 0.3 to 5.3, meaning that migration rate is higher than or similar to the characteristic growth rate considered in this simulations  $r=0.1$ , providing a significant contribution to population recoveries. (Panel C) Extinction threshold,  $\sigma_{extinction}$ , as a function of the ratio between the characteristic dispersal distance and the spatial scale of synchrony of environmental fluctuations,  $l_m/l_e$ , using the same color codes as the previous panels, all with  $m=1$  and  $A=0.1$ . (Panel D) Scaling of the extinction threshold at large dispersal rate verified plotting the ratio  $\sigma_{extinction}/\sqrt{m}$  versus the dispersal rate  $m$  for Allee thresholds  $A=0.1$  (black),  $A=0.35$  (green), and  $A=0.6$  (purple) obtained for the mean-field approximation. For all the panels in the figure, we have considered a growth rate  $r=1$  and a carrying capacity  $K=1$ .

From the mean-field approximation, we get that in the absence of dispersal,  $m=0$ , the population probability, Eq. 5, diverges in  $N=0$  as  $N^{-2(1+\frac{r}{\sigma^2})}$ , indicating that the population always goes extinct (after a certain transition time). However, when dispersal is present, the dispersal term with  $I$  suppress the divergence at zero population density, and species can be sustained, then, migration is necessary to sustain a population at long times. This result is consistent with previous results found with a constant migration term in (Dennis et al. 2016), where a similar study as ours was done but considering a constant external migration in the growth equation instead of spatial extended diffusion within the habitat. In the case with dispersal, the system of equations formed by Eqs. 5 and 6 is numerically found to have two roots or no root. (See Fig. 2A.) The two regimes are separated by a critical value of the amplitude of environmental fluctuations,  $\sigma_{extinction}$ . (The results obtained with the mean-field approximation are shown with black dots in Fig. 3.) For values above this extinction threshold,  $\sigma_{extinction}$ , populations get extinct in all the locations. In contrast, for values below the extinction threshold, there is an equilibrium

between extinction and recovery from extinction due to dispersal from other regions. The two branches of solutions represent two different equilibria. The high mean population density solution,  $p_{\text{high}}$  (green curves in Panels B, D, and F of Fig. 1) has most regions of space with population densities above the Allee threshold, and local extinction is rare. The regions above the Allee threshold have population densities below the carrying capacity due to the cost of recovering areas with local extinction. The low mean value solution  $p_{\text{low}}$  (red curves in Panels B, D, and F of Fig. 1) has most of the regions below the Allee threshold, and they are just prevented from extinction due to the dispersal contributions from the regions with population densities above the Allee threshold. These two ideal solutions have been obtained in the mean-field approximation, which assumes large dispersal lengths ( $l_m \gg l_e$ ); nonetheless, this approximation is a limit case that can be useful to understand populations with shorter dispersal lengths, because their extinction thresholds have a similar dependence with the change of parameters (Figures 3A and 3B). Simulations with finite dispersal lengths (Fig. 1), a much more common situation, show that this two types of solutions may be present at different regions of the same habitat, and together with regions of extinction (regions of zero population density in Panel E of Fig. 1, reflected as peaks at zero in the histogram of Panel F of Fig. 1).

The additional maximum approximation explained in the methods section works well for low values of  $A$ , reproducing the results of the mean-field approximation ( $l_m \gg l_e$ ), as shown in Fig. 3.

On the one hand, the extinction threshold is found to decrease as the Allee threshold increases (Panel A of Fig. 3), as both simulations and mean-field approximation shows. On the other hand, increasing the dispersal rate increases the extinction threshold, which at large values of the dispersal rate grows as

$$\sigma_{extinction} \sim \sqrt{m}, \quad (8)$$

as we expected from Eq. 7, obtained by the mean-field and maximum approximation (See Panels B and D of Fig. 3.). This dependence of the extinction threshold with the square root of the migration rate is related to the stochastic nature of the environmental fluctuations (which is here modelled with a Weiner process). Finally, maximum values of the extinction threshold are found in the mean-field limit, where characteristic dispersal distance is much larger than the spatial scale of environmental synchrony,  $l_m \gg l_e$  (right-hand side of Panel C of Fig. 3). For values of the dispersal distance of the order of the spatial scale of environmental synchrony, the extinction threshold is reduced (for example, to half the value given by the mean-field approximation in the simulation shown in the blue dots of Panel C of Fig. 3). Therefore, resilience to environmental noise is reduced when dispersal is less frequent (lower  $m$ ) or more local (lower  $l_m$ ).

#### 4. Discussion

We have shown that dispersal can make a population with an Allee threshold more resilient to environmental noise-induced extinction. This resilience can be characterized by the extinction threshold  $\sigma_{extinction}$  for the amplitude of environmental fluctuations, above which the species gets extinct. This extinction threshold increases if the dispersal rate  $m$  increases, or if the relative dispersal length  $l_m/l_e$  increases. Mean-field approximation leads us to identify two branches of sustainable population distributions. For one of the branches, high-density population state, the population distribution has most regions above the Allee threshold and some regions below it. (See blue curve in Fig. 1F.) For the other branch, low-density population state, the population distribution has most regions with a population below the Allee threshold but sustained by dispersal from the regions above the Allee threshold. (See red curve in Fig. 1F.) Dennis et al. (Dennis et al. 2016) already identified the two branches, of low and high population densities,

but for one location with external migration. Here, this analysis has been done for a spatially extended population with only internal dispersal. This means that regions with local extinction can be recolonized through dispersal from neighboring populations. We also show here that the path to global extinction is a path through the emergence of local depletions and extinctions, which spatially coexist with non-depleted regions (even in homogeneous habitats). In this path to global extinction, low-density and extinct regions cover larger and larger fraction of the area as the amplitude of environmental fluctuations increases towards the extinction threshold.

The low-density population state found may be related to the absence of recovery seen in some ecosystems after halting harvesting (Lotze et al. 2011). In those ecosystems, the species seems to be trapped in a low-density population state, where they have been lead by harvesting, but they do not recover to the previous high-density population state despiste harvesting is stopped during long periods. Further studies of transitions between low and high-density population states have to be done to deeply understand the implications of the two states presented here for these ecosystems. Our current results already suggest that the repopulation of an area can lead to a change from the low to the high-density population state, but that the repopulation should be intense enough to lead to a change in the regime of the dynamics in this area. Further studies could provide additional clues to optimize repopulation strategies. It would be also interesting to address the particular case where the Allee effect arises as a consequence of a population density dependent mating rate, as in the studies in two dimensional habitats done in (Windus & Jensen 2007, Pires & Queiros 2019).

Our results provide a new tool for the assessment of extinction risk under an increase of the amplitude of environmental fluctuations, for example, the increase in climate variability reported for several regions of the Earth (IPCC 2012). The two branches of solutions identified, high and

low-density population states, require a future detailed analysis of transitions between them and to extinction, and factors that influence these transitions, like harvesting and habitat suitability (which in nature are generally heterogeneous and stochastic in space and time). These analysis in the theoretical framework proposed here will provide information on the resilience of the high and low-density population states in finite-size habitats, assessing the impact of these states and transitions for the species sustainability on a scenario of increasing climate variability (IPCC 2012).

This theoretical framework also allows to study the impact of fragmentation (i.e., the effects of having finite size habitats), which introduces an effective limit in the dispersal. Therefore, fragmentation is expected to reduce the potential of dispersion to recover populations and lead to a reduction of the resilience to environmental fluctuations.

### *Acknowledgments*

We would like to acknowledge Javier Jarillo for help with the simulation code, and Daniel Oro and Bernt-Erik Saether for comments on the manuscript.

### *Funding*

This work was supported by the European Economic Area (EEA) Grants UCM-EEA-ABEL-02-2009 and 005-ABEL-CM2014A under the NILS – Science and Sustainability Programme, by the SUSTAIN and SFF-III 223257/F50 projects of the Research Council of Norway. FJCG acknowledge financial support through grants, FIS2010-17440 and FIS2006-05895 of Ministerio de Ciencia e Innovación (Spain), FIS2015-67745-R (MINECO/FEDER) and RTI2018-095802-B-I00 of Ministerio de Economía y Competitividad (Spain) and Fondo Europeo de Desarrollo

Regional (FEDER, EU), GR35/14-920911, GR35/10-A-920911 and GR58/08-920911 of Universidad Complutense de Madrid and Banco Santander (Spain).

## *References*

- Allee, W. C. 1931. *Animal Aggregations. A Study in General Sociology*. Chicago: The University of Chicago Press. <https://doi.org/10.5962/bhl.title.7313>.
- Allee, W. C., and G. M. Rosenthal. 1949. "Group Survival Value for *Philodina Rosola*, A Rotifer." *Ecology* 30 (3): 395–97. <https://doi.org/10.2307/1932623>.
- Angulo, Elena, Gary W. Roemer, Luděk Berec, Joanna Gascoigne, and Franck Courchamp. 2007. "Double Allee Effects and Extinction in the Island Fox." *Conservation Biology*. <https://doi.org/10.1111/j.1523-1739.2007.00721.x>.
- Bonsall, Michael B., Claire A. Dooley, Anna Kasparson, Tom Brereton, David B. Roy, and Jeremy A. Thomas. 2014. "Allee Effects and the Spatial Dynamics of a Locally Endangered Butterfly, the High Brown Fritillary (*Argynnis Adippe*)." *Ecological Applications*. <https://doi.org/10.1890/13-0155.1>.
- Dennis, Brian. 2002. "Allee Effects in Stochastic Populations." *Oikos*. <https://doi.org/10.1034/j.1600-0706.2002.960301.x>.
- Dennis, Brian, Laila Assas, Saber Elaydi, Eddy Kwessi, and George Livadiotis. 2016. "Allee Effects and Resilience in Stochastic Populations." *Theoretical Ecology* 9 (3): 323–35. <https://doi.org/10.1007/s12080-015-0288-2>.
- Engen, Steinar, Russell Lande, and Bernt Erik Sæther. 2003. "Demographic Stochasticity and Allee Effects in Populations with Two Sexes." *Ecology* 84 (9): 2378–86.

<https://doi.org/10.1890/02-0123>.

Frankham, Richard, and Katherine Ralls. 1998. “Inbreeding Leads to Extinction.” *Nature*.

<https://doi.org/10.1038/33022>.

Hackney, E. E., and J. B. McGraw. 2001. “Experimental Demonstration of an Allee Effect in

American Ginseng.” *Conservation Biology*. [https://doi.org/10.1046/j.1523-](https://doi.org/10.1046/j.1523-1739.2001.98546.x)

[1739.2001.98546.x](https://doi.org/10.1046/j.1523-1739.2001.98546.x).

IPCC. 2012. *Managing the Risks of Extreme Events and Disasters to Advance Climate Change*

*Adaptation*. Edited by Christopher B. Field, Vicente Barros, Thomas F. Stocker, Qin Dahe,

David Jon Dokken, Kristie L. Ebi, Michael D. Mastrandrea, et al. *Managing the Risks of*

*Extreme Events and Disasters to Advance Climate Change Adaptation*.

<https://doi.org/10.1017/cbo9781139177245>.

Jarillo, Javier, Bernt Erik Sæther, Steinar Engen, and Francisco J. Cao. 2018. “Spatial Scales of

Population Synchrony of Two Competing Species: Effects of Harvesting and Strength of

Competition.” *Oikos* 127 (10): 1459–70. <https://doi.org/10.1111/oik.05069>.

Karlin, Samuel, and Howard M Taylor. 1967. *A First Course in Stochastic Processes 2nd Ed.*

*SIAM Review*. <https://doi.org/10.1137/1009056>.

Kenward, R. E. 2006. “Hawks and Doves: Factors Affecting Success and Selection in Goshawk

Attacks on Woodpigeons.” *The Journal of Animal Ecology*. <https://doi.org/10.2307/3793>.

Kuparinen, Anna, and Jeffrey A. Hutchings. 2014. “Increased Natural Mortality at Low

Abundance Can Generate an Allee Effect in a Marine Fish.” *Royal Society Open Science* 1

(2): 140075–140075. <https://doi.org/10.1098/rsos.140075>.

- Law, R, U Dieckmann, and JAJ Metz. 2000. "Introduction." In *The Geometry of Ecological Interactions: Simplifying Spatial Complexity*, edited by U Dieckmann, R Law, and JAJ Metz, 1–6. Cambridge University Press.  
<http://www.iiasa.ac.at/~dieckman/reprints/LawEtal2000.pdf>.
- Lee, Aline Magdalena, Bernt-Erik Sæther, and Steinar Engen. 2011. "Demographic Stochasticity, Allee Effects, and Extinction: The Influence of Mating System and Sex Ratio." *The American Naturalist* 177 (3): 301–13. <https://doi.org/10.1086/658344>.
- Lewis, M.A., and P. Kareiva. 1993. "Allee Dynamics and the Spread of Invading Organisms." *Theoretical Population Biology* 43 (2): 141–58. <https://doi.org/10.1006/TPBI.1993.1007>.
- Liebhold, Andrew, and Jordi Bascompte. 2003. "The Allee Effect, Stochastic Dynamics and the Eradication of Alien Species." *Ecology Letters* 6: 133–40.
- Lotze, Heike K, Marta Coll, Anna M Magera, Christine Ward-paige, and Laura Airoidi. 2011. "Recovery of Marine Animal Populations and Ecosystems" 26 (11): 595–605.  
<https://doi.org/10.1016/j.tree.2011.07.008>.
- Méndez, Vicenç, Michael Assaf, Axel Masó-Puigdellosas, Daniel Campos, and Werner Horsthemke. 2019. "Demographic Stochasticity and Extinction in Populations with Allee Effect." *Physical Review E* 99 (2): 022101. <https://doi.org/10.1103/PhysRevE.99.022101>.
- Molnár, Péter K., Andrew E. Derocher, Mark A. Lewis, and Mitchell K. Taylor. 2008. "Modelling the Mating System of Polar Bears: A Mechanistic Approach to the Allee Effect." *Proceedings of the Royal Society B: Biological Sciences*.  
<https://doi.org/10.1098/rspb.2007.1307>.

- Morozov, Andrew, and Jean Christophe Poggiale. 2012. "From Spatially Explicit Ecological Models to Mean-Field Dynamics: The State of the Art and Perspectives." *Ecological Complexity* 10: 1–11. <https://doi.org/10.1016/j.ecocom.2012.04.001>.
- Moynihan, Martin H., and H. Kruuk. 2010. "Predators and Anti-Predator Behaviour of the Black-Headed Gull (*Larus Ridibundus* L.)." *Bird-Banding*.  
<https://doi.org/10.2307/4511169>.
- Odum, Howard T., and W. C. Allee. 2006. "A Note on the Stable Point of Populations Showing Both Intraspecific Cooperation and Disoperation." *Ecology*.  
<https://doi.org/10.2307/1931412>.
- Ralls, Katherine, Richard Frankham, and Jonathan D. Ballou. 2013. "Inbreeding and Outbreeding." In *Encyclopedia of Biodiversity: Second Edition*.  
<https://doi.org/10.1016/B978-0-12-384719-5.00073-3>.
- Saether, Bernt-Erik, Thor Harald Ringsby, Eivin Roskaft, Eivin Røskaft, and Bernt-Erik Sæther. 2006. "Life History Variation, Population Processes and Priorities in Species Conservation: Towards a Reunion of Research Paradigms." *Oikos*. <https://doi.org/10.2307/3546060>.
- Vercken, E., A. M. Kramer, P. C. Tobin, and J. M. Drake. 2011. "Critical Patch Size Generated by Allee Effect in Gypsy Moth, *Lymantria Dispar* (L.)." *Ecology Letters* 14 (2): 179–86.  
<https://doi.org/10.1111/j.1461-0248.2010.01569.x>.
- Way, M. J., and C. J. Banks. 1967. "Intra-Specific Mechanisms in Relation to the Natural Regulation of Numbers of *Aphis Fabae* Scop." *Annals of Applied Biology* 59 (2): 189–205.  
<https://doi.org/10.1111/j.1744-7348.1967.tb04428.x>.

